ACS OMEGA

http://pubs.acs.org/journal/acsodf

Article

Surface-Modified TiO_2@SiO_2 Nanocomposites for Enhanced Dispersibility and Optical Performance to Apply in the Printing Process as a Pigment

Lei Wang,* Guangyuan Xie, Xiang Mi,* Bin Zhang, Yu Du, Qiuyu Zhu, and Zhicheng Yu

Cite This: *ACS Omega* 2023, 8, 20116−20124

Read Online

ACCESS | Metrics & More | Article Recommendations

ABSTRACT: The grafted modification TiO_2@SiO_2 composite was fabricated by a liquid-phase deposition method with Na_2SiO_3 and a grafting reaction with a silane coupling agent. First, the TiO_2@SiO_2 composite was prepared, and the effect of deposition rate and silica content on the morphology, particle size, dispersibility, and pigmentary property of TiO_2@SiO_2 composites was investigated by scanning electron microscopy (SEM), transmission electron microscopy (TEM), Fourier transform infrared (FTIR) spectroscopy, energy-dispersive X-ray spectroscopy (EDX), X-ray photoelectron spectroscopy (XPS), and ζ-potential. The islandlike TiO_2@SiO_2 composite had a good particle size and printing performance compared with the dense TiO_2@SiO_2 composite. The presence of Si was confirmed by EDX elemental analysis and XPS, and a peak at 980 cm^{-1} belonging to Si−O was observed in the FTIR spectrum, confirming the presence of SiO_2 anchored at TiO_2 surfaces via Si−O−Ti bonds. Then, the islandlike TiO_2@SiO_2 composite was modified by grafting with a silane coupling agent. The effect of the silane coupling agent on the hydrophobicity and dispersibility was investigated. The peaks at 2919 and 2846 cm^{-1} belong to CH_2 in the FTIR spectrum, and Si−C in the XPS confirmed the grafting of silane coupling agent to the TiO_2@SiO_2 composite. The grafted modification of the islandlike TiO_2@SiO_2 composite using 3-triethoxysilylpropylamine endowed it with weather durability, dispersibility, and good printing performance.

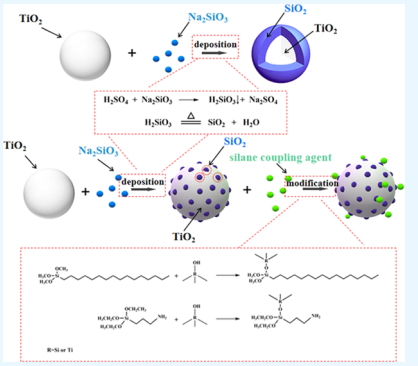

1. INTRODUCTION

Titanium dioxide (TiO_2) is the best white pigment due to its excellent optical properties, which is widely used in coatings, plastics, paper, ink, and other industries. However, TiO_2 particles generate electrons and holes under ultraviolet light and then react with water and oxygen to generate free radicals, which leads to the degradation of organic matter around the TiO_2 particles.[1−4] The photocatalytic performance of TiO_2 causes defects such as breakage and yellowing of the adhesive. In order to increase the weather resistance of TiO_2 particles, the surface of TiO_2 particles was coated with an inert oxide barrier film, such as silica and alumina.[5,6] A liquid-phase deposition method was usually used for inorganic thin-film coating. By adding the inorganic salt and acid/alkali solution to the TiO_2 suspension, a layer of oxide or hydroxide film was coated on the surface of the TiO_2 particles, which increased the weather resistance of the TiO_2 particles.[7,8] The SiO_2 coating layers increased the amount of OH groups on the surfaces of TiO_2 particles, which improved the dispersibility of TiO_2 particles in aqueous media and provided more active sites for the subsequent organic modification.[9,10] Zhang et al. used zirconium dioxide to coat TiO_2, and the prepared TiO_2@ZrO_2 had good weather resistance, whiteness, and brightness.[11]

Although the coating of inorganic metal oxide on the surface of TiO_2 inhibited the photocatalytic performance of TiO_2, the refractive index of inorganic metal oxide was lower than that of TiO_2, resulting in the decrease of covering performance of inorganic metal oxide-coated titanium dioxide particles. Liang et al. applied inorganic metal oxides to coat TiO_2 to improve the weather resistance of TiO_2. The results showed that the coating of dense films of inorganic metal oxides greatly reduced the covering properties of TiO_2.[12] Wang et al. found that the use of a yolk−shell structure and a porous film could solve the problems of poor weather resistance and reduced the covering performance of inorganic oxide-coated titanium dioxide.[13]

In the titanium dioxide printing paste formula, the amount of TiO_2 was very high and it was insoluble in water so the aggregation of TiO_2 in the printing paste formula could easily occur. When the titanium dioxide aggregated, its increased

Received: April 19, 2023
Accepted: May 9, 2023
Published: May 19, 2023

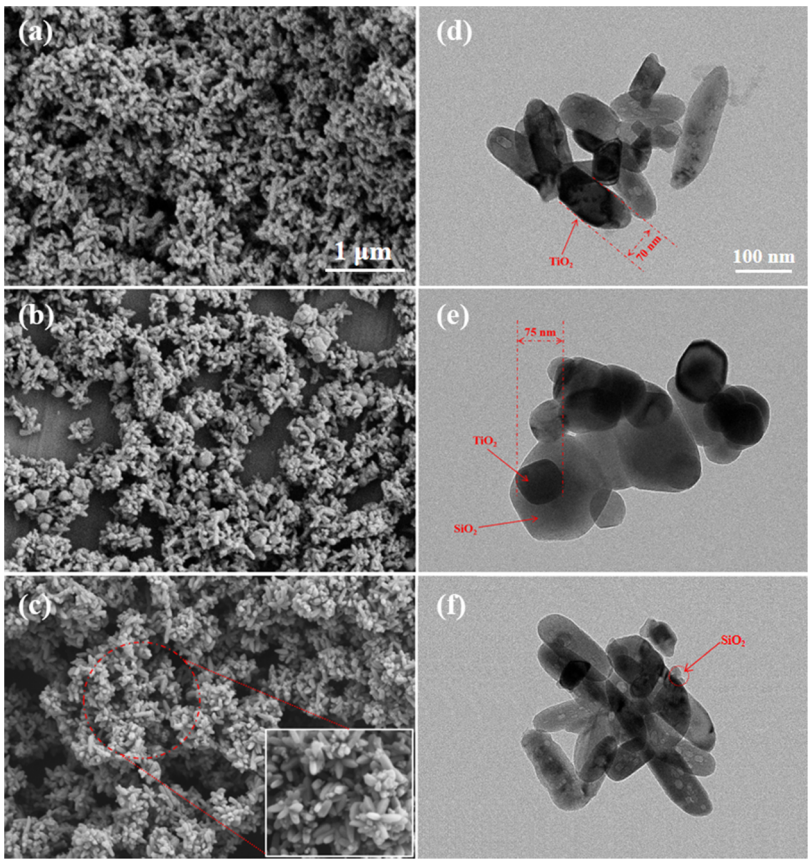

Figure 1. SEM images: (a) naked TiO_2, (b) dense TiO_2@SiO_2, and (c) islandlike TiO_2@SiO_2. TEM images: (d) naked TiO_2, (e) dense TiO_2@SiO_2, and (f) islandlike TiO_2@SiO_2.

particle size reduced its optical properties. In order to improve the dispersibility of TiO_2, a lot of studies have been carried out, among which the chemical modification of TiO_2 was a more effective method.[14] The silane coupling agents were applied to the chemical modification of inorganic particulates, improving the stability and dispersibility.[15] Wang et al. used γ-methacrylic acyloxy propyl trimethoxysilane to chemically modify TiO_2, which changed the hydrophobicity of TiO_2 and improved the dispersion stability.[16] The thermoplastic resin was used to improve the stability and dispersibility of pigment by chemical modification.[17]

In this study, the TiO_2 pigment was coated with an islandlike or dense structure of silica by controlling the precipitation rate of SiO_2. The effect of precipitation rate and silica content on the morphology, ζ-potential, particle size, dispersibility, and pigment property of TiO_2@SiO_2 composites was investigated. To further improve the dispersibility and printing performance, the TiO_2@SiO_2 composite was subjected to chemical modification with silane coupling agents by ultrasound treatment. The chemical structure of the grafted modification TiO_2@SiO_2 composites was analyzed in detail. For coating treatment and hydrophilic modification, the printing performance of hydrophilic modification TiO_2@SiO_2 composites was improved.

2. MATERIALS AND METHODS

2.1. Materials. The 40 s × 40 s plain-woven pure cotton fabric (weighing 116 g/m^2) was provided by Hualun Co., Ltd. The TiO_2, sodium metasilicate nonahydrate, sodium hexametaphosphate, 3-triethoxysilylpropylamine (APTES), sulfuric acid, and ammonia were obtained from Shanghai Aladdin Biochemical Technology Co., Ltd. The acrylic binder, acrylic thickener, and dispersant were provided by Zhejiang Transchem Chemical Group. The hexadecyltrimethoxysilane (HDTMS) and rhodamine-B were obtained from Macklin Inc.

2.2. Process of Preparing TiO_2@SiO_2 and Grafted Modification TiO_2@SiO_2. *2.2.1. Preparing the TiO_2@SiO_2 Composite.* The surface of TiO_2 nanoparticles was coated with SiO_2 nanoparticles. First, TiO_2 nanoparticles (20 g) and sodium hexametaphosphate (0.1 g) were dispersed in 80 mL of deionized water with the aid of ultrasonication for 30 min in the solution of pH = 9−10, and the solution was stirred vigorously for 30 min. Next, a certain amount of sodium metasilicate nonahydrate (0.3 mol/L) was injected into the mixture using a syringe pump at a rate of 1.0 or 4.0 mL/min at 85 °C. At the same time, the pH of the solution was maintained by adding H_2SO_4 (1.6 wt %). After injecting, the resulting TiO_2@SiO_2 particles were centrifuged, washed 3−5 times with ethanol, dried under vacuum, and ground.

2.2.2. Surface Grafting Modification of TiO_2@SiO_2 Particles. The surface of the TiO_2@SiO_2 composite was subjected to grafting modification with APTES or HDTMS. The TiO_2@SiO_2 composite (10 g) was dispersed in a mixture of sodium hexametaphosphate (0.4 g), ammonia (1.5 g), and deionized water (150 mL). After stirring for 30 min, APTES or HDTMS (10 wt %) was injected into the mixture. Then, the solution was sonicated and stirred vigorously for 4 h. After sonicating and stirring, the resulting grafted modification TiO_2@SiO_2 composites were centrifuged, washed 3−5 times with ethanol, dried under vacuum, and ground.

https://doi.org/10.1021/acsomega.3c02679
ACS Omega 2023, 8, 20116−20124

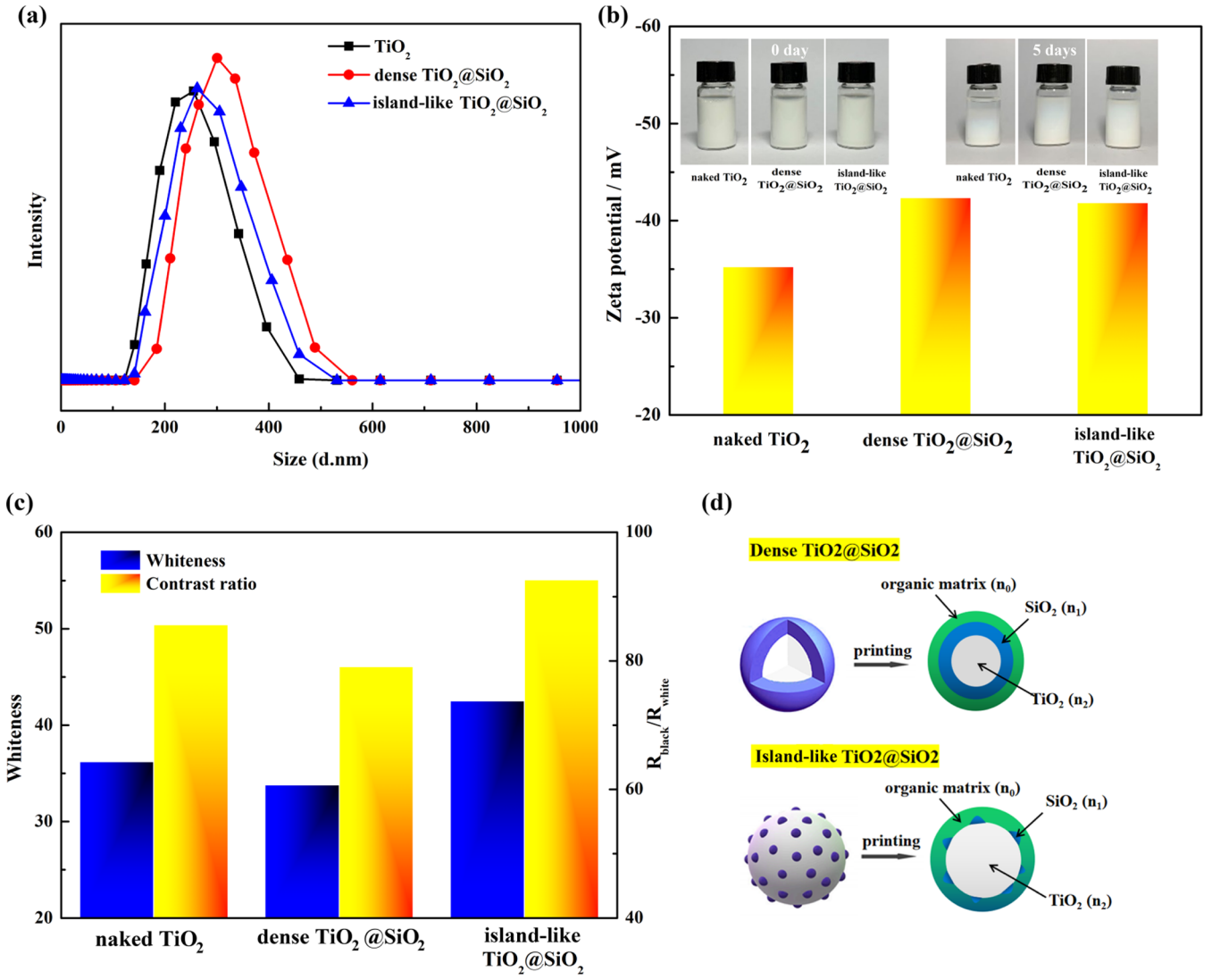

Figure 2. (a) Particle size of the naked TiO_2, dense TiO_2@SiO_2 composite, and islandlike TiO_2@SiO_2 composite. (b) Dispersion stability and ζ-potential of different particles. (c) Printing performance of different particles, and (d) schematic diagram of the TiO_2@SiO_2 composite.

2.3. Process of Printing Cotton Fabric. First, a proper amount of binder, dispersant, and TiO_2 particles was added to water to form a dispersion system, which was stirred evenly under a mechanical stirrer (1000 rpm). Then, the thickener was slowly added to it to make the printing paste with a certain viscosity. The printing paste formula was printed on the cotton fabric; then, the sample was dried at 80 °C for 5 min and baked at 150 °C for 5 min.

2.4. Analysis and Measurements. *2.4.1. ζ-Potential Measurement.* The sample was diluted to a certain concentration and prepared as a suspension. The sample was put into the ζ-potential analyzer to measure the ζ-potential.

2.4.2. Particle Size Measurement. The sample was diluted to a certain concentration and prepared as a suspension, which was put into a nanoparticle sizer to measure the particle size.

2.4.3. SEM, EDX, and TEM Measurement. The sample was dispersed in deionized water; then, the sample was treated by ultrasound for 20 min. The sample was observed with a field-emission scanning electron microscope equipped with an energy-dispersive X-ray spectrometer (S-4800, Hitachi, Japan) and TEM (H-9500, Hitachi, Japan).

2.4.4. X-ray Photoelectron Spectroscopy. The chemical composition of the particle was examined by X-ray photoelectron spectrometry (XPS, Thermo ESCALAB 250).

2.4.5. ATR-FTIR Spectroscopy. The attenuated total reflectance-Fourier transform spectroscopy (ATR-FTIR) spectra of the sample were recorded on a Spectrum II (PerkinElmer) in the range of 4000−400 cm^{-1}.

2.4.6. Contact Angle Measurement. The hydrophobic property of particle was measured via an optical contact angle meter system (DSA100, Germany).

2.4.7. Printing Performance and Weather Durability Measurement. The printed sample was measured by a Datacolor 650 to obtain the reflectance of blackboard and whiteboard printed by printing paste formula. The contrast ratio was the ratio of the reflectivity of the blackboard and the whiteboard. The whiteness of printed cotton fabrics was measured by WSB-2 intelligent whiteness tester. Weather durability measurement was referred from a previous research.[13]

https://doi.org/10.1021/acsomega.3c02679
ACS Omega 2023, 8, 20116−20124

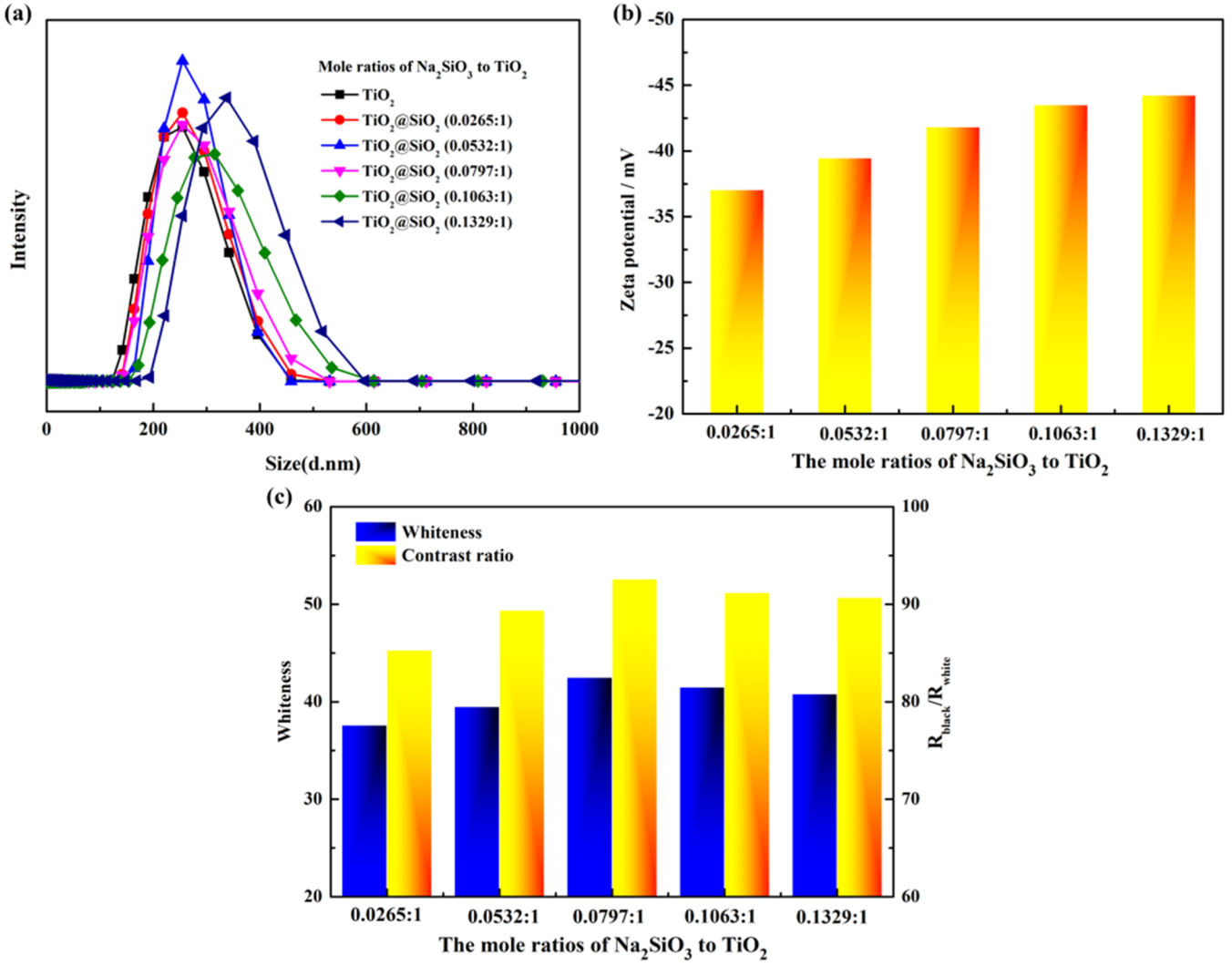

Figure 3. Effect of mole ratios of Na_2SiO_3 to TiO_2 on the particle size (a), ζ-potential (b), and printing performance (c) of the islandlike TiO_2@SiO_2 composite.

3. RESULTS AND DISCUSSION

3.1. Synthesis and Characterization of TiO_2@SiO_2. The TiO_2@SiO_2 composite was prepared via a liquid-phase deposition method with Na_2SiO_3. The deposition rate controlled by the drip rate of Na_2SiO_3 and H_2SO_4 was a significant factor that influenced the morphology of TiO_2@SiO_2. As seen in Figure 1a,d, the naked TiO_2 was a rod structure with a length of about 240 nm and a width of about 70 nm. With the deposition of SiO_2 on the surface of TiO_2 at a faster drip rate of Na_2SiO_3 and H_2SO_4 (4.0 mL/min), the obvious dense spherical SiO_2-coated rodlike TiO_2 composite was formed (shown in Figure 1b,e). As shown in Figure 1e, the size of this composite was increased compared with naked TiO_2. When the drip rate of Na_2SiO_3 and H_2SO_4 was slow (1.0 mL/min), the deposition rate of SiO_2 on the surface of TiO_2 was also decreased accordingly so that the morphology of TiO_2@SiO_2 was different from TiO_2@SiO_2 at a faster drip rate (4.0 mL/min). As seen from Figure 1c,f, the islandlike layer of SiO_2 on the surface of TiO_2 was prepared.

The morphology of TiO_2@SiO_2 prepared by different drip rates was different due to the deposition rate of SiO_2 on the surface of TiO_2. In the liquid-phase deposition method, the TiO_2 particle acted as a crystal nucleus and the generation of SiO_2 grew on its surface. At a faster drip rate of Na_2SiO_3 and H_2SO_4, SiO_2 was generated quickly and a larger amount of SiO_2 was deposited on the TiO_2 particle to prepare dense TiO_2@SiO_2. However, at a slow drip rate, generated SiO_2 was randomly deposited on the surface of TiO_2 to obtain islandlike TiO_2@SiO_2.

Figure 2a shows the particle size, dispersion stability, and ζ-potential of the naked TiO_2, dense TiO_2@SiO_2, and islandlike TiO_2@SiO_2. As seen in Figure 2a, the average particle size of naked TiO_2, dense TiO_2@SiO_2, and islandlike TiO_2@SiO_2 was 253, 318, and 286 nm, respectively. The size of dense TiO_2@SiO_2 increased obviously compared with naked TiO_2. The dispersion stability of TiO_2@SiO_2 after 5 days improved due to the decrease of ζ-potential, which contributed to the electrostatic stabilization of TiO_2@SiO_2 composites compared with naked TiO_2 (shown in Figure 2b). As seen in Figure 2c, the whiteness of printed cotton fabric and contrast ratio using naked TiO_2 were 36.2 and 85.6%, respectively. Compared with naked TiO_2, the whiteness and contrast ratio using dense TiO_2@SiO_2 declined, and the whiteness and contrast ratio using islandlike TiO_2@SiO_2 were increased to 42.5 and 92.6%, respectively. The hiding power was related to the square of the difference between the refractive index of the pigment and the

https://doi.org/10.1021/acsomega.3c02679
ACS Omega 2023, 8, 20116−20124

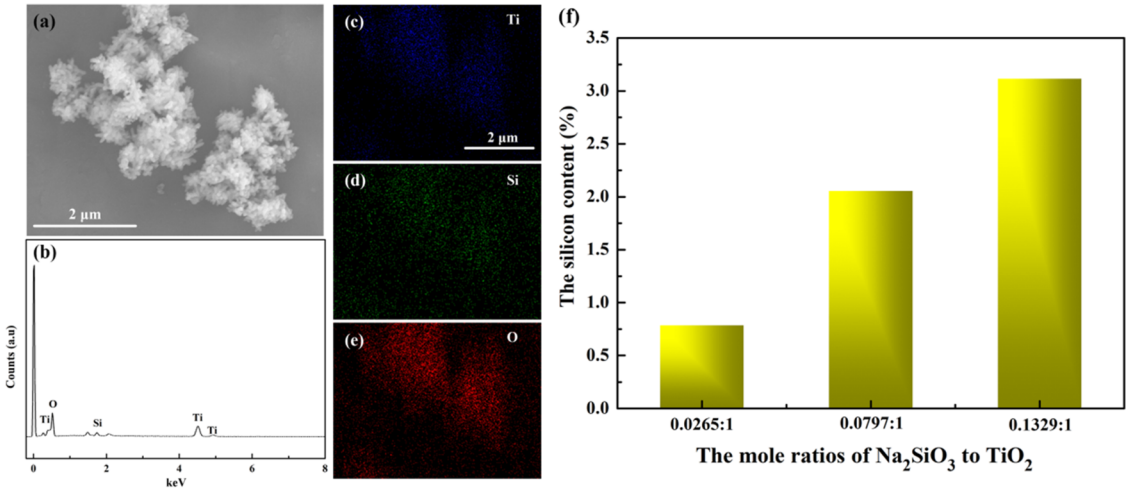

Figure 4. (a) SEM images of the islandlike TiO_2@SiO_2 composite. (b) EDX spectroscopy of the islandlike TiO_2@SiO_2 composite. (c–e) Elemental mapping of Ti, Si, and O, and (f) silicon content of the islandlike TiO_2@SiO_2 composite.

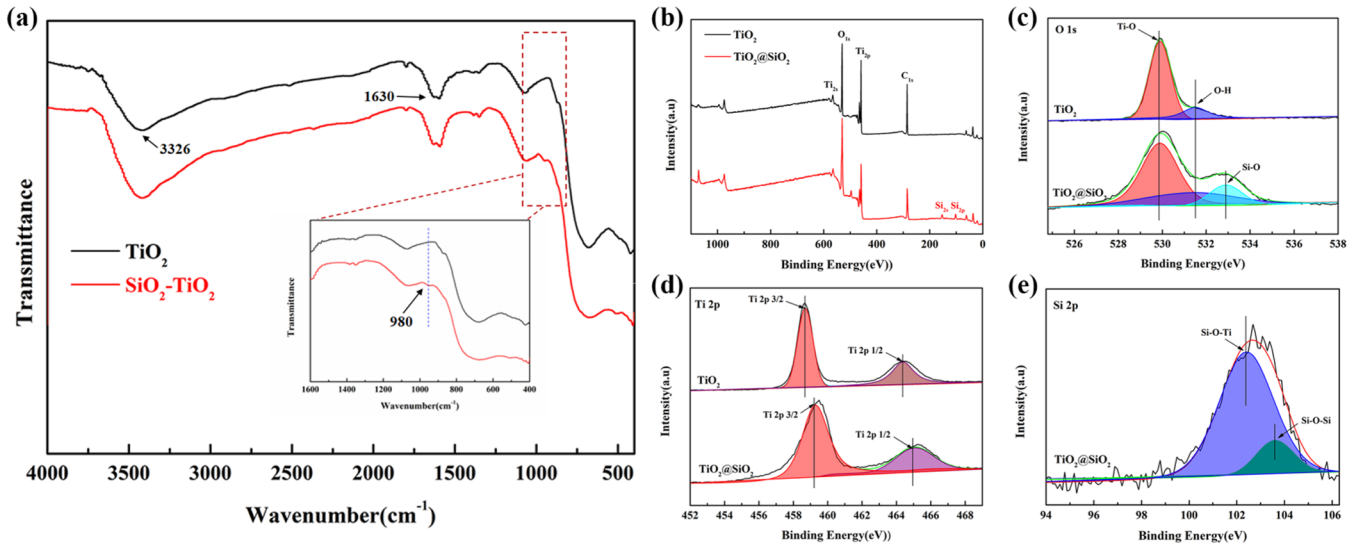

Figure 5. (a) FTIR spectrum of the naked TiO_2 and the islandlike TiO_2@SiO_2 composite. (b) Representative XPS spectra of the naked TiO_2 and islandlike TiO_2@SiO_2 composite. (c–e) High-resolution XPS spectra of O 1s, Ti 2p, and Si 2p.

organic matrix. Theoretically, naked TiO_2 particles had high hiding performance due to the high difference of refractive index between TiO_2 particles and its surroundings. For the TiO_2@SiO_2 composite, the surrounding was the SiO_2 film (n_1) instead of an organic matrix (n_0) (shown in Figure 2d). The difference of refractive indices between SiO_2 particle (n_1) and organic matrix (n_0) was lower than the difference of refractive indices between TiO_2 particle (n_2) and organic matrix (n_0) so that the hiding power of the dense TiO_2@SiO_2 composite declined. For the islandlike TiO_2@SiO_2 composite, the surrounding of TiO_2 particle was partly replaced by SiO_2 particle compared with the dense TiO_2@SiO_2 composite so that the difference of refractive indices was not declined obviously. In addition, the deposition of SiO_2 particle on the surface of TiO_2 particle, increasing the ζ-potential of the TiO_2@SiO_2 composite, contributed to the dispersibility of the TiO_2@SiO_2 composite in the printing formula so that the hiding performance of the islandlike TiO_2@SiO_2 composite was improved. Therefore, the islandlike TiO_2@SiO_2 composite is discussed in the following section.

The effect of mole ratios of Na_2SiO_3 to TiO_2 on the particle size, ζ-potential, and printing performance of the islandlike TiO_2@SiO_2 composite is shown in Figure 3. As seen in Figure 3a,b, with the increase of mole ratios of Na_2SiO_3 to TiO_2 from 0.0265:1 to 0.1329:1, the average particle size increased from 262 to 350 nm, and the ζ-potential decreased from −38.2 to −43.8 mV. As shown in Figure 3c, with an increase of mole ratios of Na_2SiO_3 to TiO_2 from 0.0265:1 to 0.0797:1, the whiteness and contrast ratio increased from 37.6 to 42.5 and from 85.3 to 92.6%, respectively. With further increase in mole ratios above 0.0797:1, the whiteness and contrast ratio declined. The reason for this phenomenon was that at higher mole ratios, the size of the islandlike TiO_2@SiO_2 composite became large and the massively deposited SiO_2 on the surface of TiO_2 resulted in the decrease of refractive indices. Therefore, the mole ratio of Na_2SiO_3 to TiO_2 of 0.0797:1 was the optimum condition to obtain the islandlike TiO_2@SiO_2 composite with good printing performance.

The chemical structure of the islandlike TiO_2@SiO_2 composite was analyzed by EDX, FTIR, and XPS in Figures 4 and 5. The EDX spectroscopy of the islandlike TiO_2@SiO_2

https://doi.org/10.1021/acsomega.3c02679
ACS Omega 2023, 8, 20116−20124

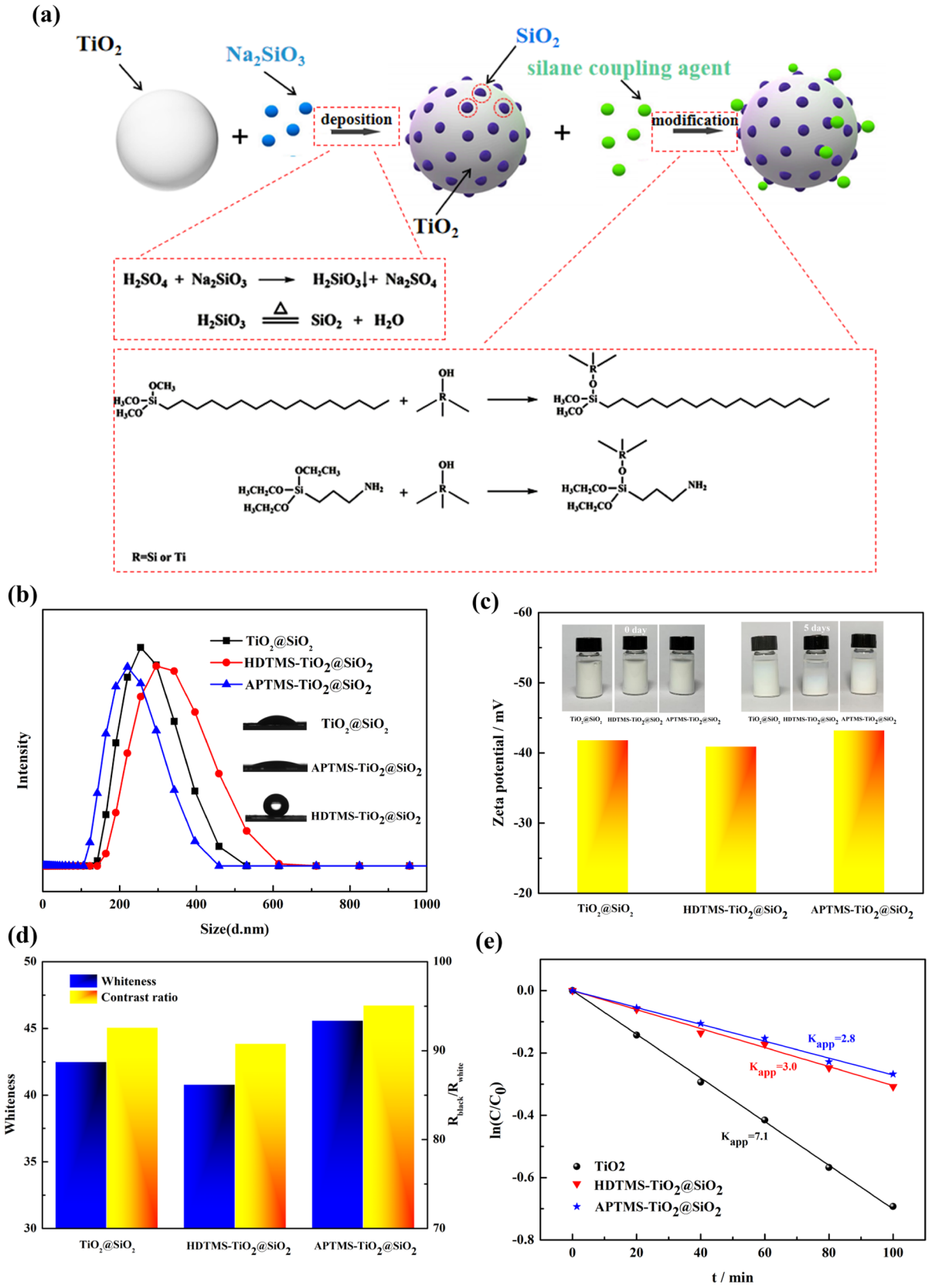

Figure 6. Synthesis process to prepare grafted modification islandlike TiO_2@SiO_2 (a). Effect of APTMS and HDTMS on the size, contact angle (b), ζ-potential, dispersibility stability (c), printing performance (d), and degradation of rhodamine-B (e) of the grafted modification TiO_2@SiO_2 composite.

composite is shown in Figure 4b, indicating that the sample was composed of the elements Ti, O, and Si. The EDX elemental mapping figure of Ti, O, and Si shown in Figure 4c–e indicated the distribution of the SiO_2 on the surface of TiO_2

https://doi.org/10.1021/acsomega.3c02679
ACS Omega 2023, 8, 20116−20124

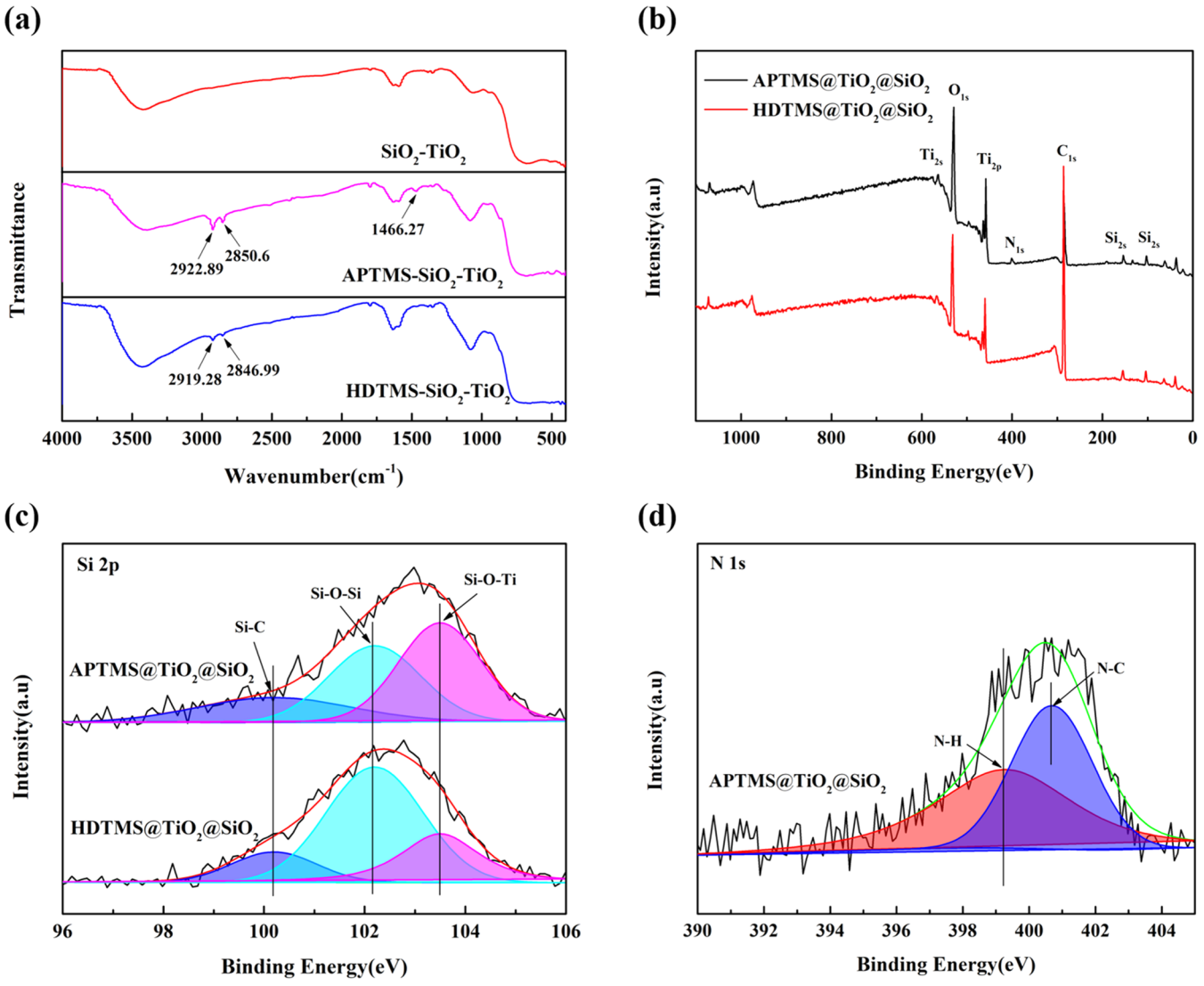

Figure 7. (a) FTIR spectrum of the islandlike TiO_2@SiO_2, APTMS-TiO_2@SiO_2, and HDTMS-TiO_2@SiO_2 composite. (b) Representative XPS spectra of the APTMS-TiO_2@SiO_2 and HDTMS-TiO_2@SiO_2 composite. (c, d) High-resolution XPS spectra of Ti 2p and N 1s.

was homogeneous. As seen in Figure 4f, with an increase of mole ratios of Na_2SiO_3 to TiO_2 from 0.0265:1 to 0.1329:1, the silicon content increased from 0.79 to 3.12%.

As seen in Figure 5a, the absorption at 3326 cm^{-1} was attributed to O−H stretching vibration,[18] and the absorption at 1630 cm^{-1} was attributed to the O−H bending vibration of adsorbed water molecules.[19] The absorption in the 400−1200 cm^{-1} exhibited characteristic peaks of O−Ti−O.[20] Compared with the naked TiO_2 particle, the islandlike TiO_2@SiO_2 exhibited a new peak at 980 cm^{-1}, which was assigned to the Si−O bond, confirming the coating of SiO_2 on the surface of TiO_2 particles.[21] Figure 5b shows representative XPS spectra of the naked TiO_2 and the islandlike TiO_2@SiO_2 composite. The obvious peaks of C 1s, Ti 2p, and O 1s appeared in the naked TiO_2 and the islandlike TiO_2@SiO_2 composite. Compared with the naked TiO_2 particle, the new peak of Si 2p appeared in the islandlike TiO_2@SiO_2 composite. To investigate the chemical composition and valence states, high-resolution XPS spectroscopy was conducted (shown in Figure 5c−e). Figure 5c shows the deconvolution of O 1s spectra. For the naked TiO_2, there were two peaks; the peak at 529.8 eV was assigned to the Ti−O bond and the peak at 531.3 eV was associated with the O−H bond.[22] Compared with the naked TiO_2, three peaks appeared in the islandlike TiO_2@SiO_2 composite. The new peak at 532.9 eV was assigned to the Si−O bond, showing the presence of SiO_2 deposited on the surface of TiO_2 particles.[23] The two peaks at 458.6 and 464.3 eV assigned to Ti $2p_{3/2}$ and Ti $2p_{1/2}$ all appeared in naked TiO_2 and the islandlike TiO_2@SiO_2 composite (shown in Figure 5d).[24] Compared with the naked TiO_2, the position of the peak in the islandlike TiO_2@SiO_2 composite was shifted, which was caused by the formation of the Si−O−Ti bond. Only the islandlike TiO_2@SiO_2 composite had two peaks at 102.2 and 103.5 eV for Si 2p, which were assigned to Si−O−Ti and Si−O−Si (seen in Figure 5e).[25] The above XPS results were in good agreement with the EDX and FTIR spectra, indicating the coating of SiO_2 on the surface of TiO_2 particles in the islandlike TiO_2@SiO_2 composite via Si−O−Ti bonds.

3.2. Grafted Modification of Islandlike TiO_2@SiO_2 and Characterization. To investigate the effect of hydrophilic properties of particle on the dispersibility and printing performance, the islandlike TiO_2@SiO_2 composite was subjected to grafted modification with APTMS and HDTMS. The synthesis process to prepare grafted modification

https://doi.org/10.1021/acsomega.3c02679
ACS Omega 2023, 8, 20116−20124

islandlike TiO_2@SiO_2 is shown in Figure 6a. Figure 6b shows the effect of APTMS and HDTMS on the size of the grafted modification TiO_2@SiO_2 composite. As seen from Figure 6b, for the HDTMS-TiO_2@SiO_2 composite, the particle size increased to 308 nm; however, the size of the APTMS-TiO_2@SiO_2 composite decreased compared with the islandlike TiO_2@SiO_2 composite. Figure 6b shows that the water contact angle of APTMS-TiO_2@SiO_2 was decreased to 15.2° and that of HDTMS-TiO_2@SiO_2 was increased to 126.2° compared with the islandlike TiO_2@SiO_2 composite (29.4°). The water contact angle was higher than 90°, indicating the particle had hydrophobic properties. The enhanced hydrophilic properties of the APTMS-TiO_2@SiO_2 composite resulted in the improvement of dispersibility so that the size of the APTMS-TiO_2@SiO_2 composite decreased. The dispersibility stability and ζ-potential of the APTMS-TiO_2@SiO_2 composite were also better than that of the islandlike TiO_2@SiO_2 or HDTMS-TiO_2@SiO_2 composite (shown in Figure 6c). The printing performance with different particles is shown in Figure 6d; the whiteness and contrast ratio using the APTMS-TiO_2@SiO_2 composite were 45.6 and 95.1%, respectively, better than that using the islandlike TiO_2@SiO_2 and HDTMS-TiO_2@SiO_2 composite. The better printing performance of the APTMS-TiO_2@SiO_2 composite was due to the improvement of dispersibility of particles in the printing formula. To improve the weather durability of TiO_2 particle, the TiO_2 particle was coated with inorganic oxide SiO_2 and then modified by grafting with a silane coupling agent. The weather durability of the TiO_2, HDTMS-TiO_2@SiO_2, and APTMS-TiO_2@SiO_2 was measured by the degradation rate of rhodamine-B. Figure 6e shows the degradation of rhodamine-B vs time for naked TiO_2, HDTMS-TiO_2@SiO_2, and APTMS-TiO_2@SiO_2 composites. As shown in Figure 6e, the degradation rate constants of rhodamine-B of the naked TiO_2, APTMS-TiO_2@SiO_2, and HDTMS-TiO_2@SiO_2 composite were 7.1, 2.8, and 3.0, respectively. Compared with the naked TiO_2, the degradation rate of HDTMS-TiO_2@SiO_2 and APTMS-TiO_2@SiO_2 was decreased so that the weather durability increased via coating of SiO_2 and grafted modification of HDTMS and APTMS. The SiO_2 particle deposited on the surface of TiO_2 hindered the generation of radicals and decreased the degradation rate of the rhodamine-B and improved the weather durability.

Figure 7 shows the FTIR and XPS spectra of islandlike TiO_2@SiO_2, APTMS-TiO_2@SiO_2, and HDTMS-TiO_2@SiO_2 composites. As seen in Figure 7a, compared with islandlike TiO_2@SiO_2, the HDTMS-TiO_2@SiO_2 composite exhibited new peaks at 2918 and 2846 cm^{-1} assigned to the C−H stretching vibration; the APTMS-TiO_2@SiO_2 composite exhibited new peaks at 2918 and 2846 cm^{-1} assigned to the C−H stretching vibration as well as 1466 cm^{-1} assigned to the C−N band.[26] Through the above FTIR results, it could be concluded that the silane coupling agent was grafted on the islandlike TiO_2@SiO_2 composite. Figure 7b shows representative XPS spectra of the islandlike TiO_2@SiO_2, APTMS-TiO_2@SiO_2, and HDTMS-TiO_2@SiO_2 composite. The obvious peaks of C 1s, O 1s, Ti 2p, and Si 2p appeared in all samples. Among these three samples, only APTMS-TiO_2@SiO_2 exhibited the characteristic peak of N 1s. The high-resolution XPS spectroscopy is shown in Figure 7c,d. As seen in Figure 7c, there were common peaks at 102.2 and 103.5 eV for the Si 2p spectra of all particles, which could be assigned to Si−O−Si and Si−O−Ti bonds. Compared with the islandlike TiO_2@SiO_2 composite, the APTMS-TiO_2@SiO_2 and HDTMS-TiO_2@SiO_2 composite had a new peak at 100.2 eV, which was attributed to the Si−C bond, indicating the grafted modification of the TiO_2@SiO_2 composite with silane coupling agent APTMS and HDTMS.[27] As seen in Figure 7d, only the APTMS-TiO_2@SiO_2 composite exhibited N 1s spectra, which could be deconvoluted to two peaks at 399.3 and 400.7 eV. The peaks at 399.3 eV were assigned to the N−H bond, and peaks at 400.7 eV were assigned to the N−C bond, suggesting the presence of APTMS on the surface of the APTMS-TiO_2@SiO_2 composite.[28]

4. CONCLUSIONS

The grafted modification SiO_2-coated TiO_2 composite was prepared by two steps: first, deposition of SiO_2 on the surface of TiO_2, followed by graft modification of the TiO_2@SiO_2 composite. The experimental results indicated that the islandlike TiO_2@SiO_2 composite conducted better printing performance due to the deposition of SiO_2 particles on the surface of SiO_2 particle homogeneously, increasing the ζ-potential of the TiO_2@SiO_2 composite to improve the dispersibility of the TiO_2@SiO_2 composite in the printing formula. Compared with the dense TiO_2@SiO_2 composite, the surrounding TiO_2 particle was partly replaced by SiO_2 particle in the islandlike TiO_2@SiO_2 composite so that the difference of refractive indices was not decreased obviously and a better printing performance was obtained. The presence of Si was confirmed by EDX elemental analysis and XPS and a peak at 980 cm^{-1} belonging to Si−O was observed in the FTIR, confirming the presence of SiO_2 anchored at TiO_2 surfaces via Si−O−Ti bonds in the islandlike TiO_2@SiO_2 composite. The islandlike TiO_2@SiO_2 composite was then modified by grafting with a silane coupling agent. The hydrophilic modification of the TiO_2@SiO_2 composite using APTMS contributed to the improvement of dispersibility and printing performance compared with hydrophobic modification using HDTMS. The grafted modification TiO_2@SiO_2 composites were characterized by FTIR and XPS. The peaks at 2919 and 2846 cm^{-1} belong to CH_2 in the FTIR spectrum and Si−C in the XPS confirmed the silane coupling agent grafted to the TiO_2@SiO_2 composite. The APTMS-TiO_2@SiO_2 composite exhibited weather durability, dispersibility, and good printing performance.

AUTHOR INFORMATION

Corresponding Authors

Lei Wang − *Engineering Research Center for Eco-Dyeing and Finishing of Textiles, Zhejiang Sci-Tech University, Hangzhou 310018 Zhejiang, China*; orcid.org/0000-0002-8783-6286; Email: wanglei90@zstu.edu.cn

Xiang Mi − *Fujian Key Laboratory of Novel Functional Textile Fibers and Materials, Clothing and Design Faculty, Minjiang University, Fuzhou 350108, China*; Email: mixiang@mju.edu.cn

Authors

Guangyuan Xie − *Engineering Research Center for Eco-Dyeing and Finishing of Textiles, Zhejiang Sci-Tech University, Hangzhou 310018 Zhejiang, China*

Bin Zhang − *Zhejiang Zhong Ding Textile Co., Ltd., Tongxiang 314500 Zhejiang, China*

Yu Du − *Engineering Research Center for Eco-Dyeing and Finishing of Textiles, Zhejiang Sci-Tech University, Hangzhou 310018 Zhejiang, China*

https://doi.org/10.1021/acsomega.3c02679
ACS Omega 2023, 8, 20116−20124

Qiuyu Zhu − *Engineering Research Center for Eco-Dyeing and Finishing of Textiles, Zhejiang Sci-Tech University, Hangzhou 310018 Zhejiang, China*
Zhicheng Yu − *Engineering Research Center for Eco-Dyeing and Finishing of Textiles, Zhejiang Sci-Tech University, Hangzhou 310018 Zhejiang, China*

Complete contact information is available at: https://pubs.acs.org/10.1021/acsomega.3c02679

Notes

The authors declare no competing financial interest.

■ ACKNOWLEDGMENTS

This work is supported by the Opening Project of China National Textile and Apparel Council Key Laboratory of Natural Dyes, Soochow University, No. SDHY2118, Talent Introduction Program of Minjiang University (MJY20030) and Guided Project of Fujian Province (2021H0056).

■ REFERENCES

(1) Maleki, H.; Bertola, V. TiO_2 nanofilms on polymeric substrates for the photocatalytic degradation of methylene blue. *ACS Appl. Nano Mater.* **2019**, *2*, 7237−7244.
(2) Wang, Y. F.; Yang, H. C.; Yun, H.; Zhang, M.; et al. Crystallization time-induced microstructural evolution and photoelectrochemical properties of ternary Ag@AgBr/TiO_2 nanorod arrays. *J. Alloys Compd.* **2022**, *904*, No. 163370.
(3) Wang, L.; Xie, G. Y.; Mi, X. A single-step pad-steam cationzation and dyeing process for improving dyeing properties of cotton fabrics. *Color. Technol.* **2022**, *138*, 509−521.
(4) Goulart, S.; Nieves, L.; Bernardin, A. Sensitization of TiO2 nanoparticles with natural dyes extracts for photocatalysis activity under visible light. *Dyes Pigm.* **2020**, *182*, No. 108654.
(5) Hakim, L. F.; King, D. M.; Zhou, Y.; et al. Nanoparticle Coating For Advanced Optical, Mechanical And Rheological Properties. *Adv. Funct. Mater.* **2007**, *17*, 3175−3181.
(6) Wei, B.-X.; Zhao, L.; Wang, T.; et al. Photo-stability of TiO2 particles coated with several transition metal oxides and its measurement by rhodamine-B degradation. *Adv. Powder Technol.* **2013**, *24*, 708−713.
(7) Zhang, Y.; Yin, H.; Wang, A.; et al. Deposition and characterization of binary Al2O3/SiO2 coating layers on the surfaces of rutile TiO2 and the pigmentary properties. *Appl. Surf. Sci.* **2010**, *257*, 1351−1360.
(8) Gao, H.; Qian, B.; Wang, T.; et al. Cerium Oxide Coating of Titanium Dioxide Pigment to Decrease Its Photocatalytic Activity. *Ind. Eng. Chem. Res.* **2014**, *53*, 189−197.
(9) Guo, J.; Benz, D.; Nguyen, T.; et al. Tuning the Photocatalytic Activity of TiO2 Nanoparticles by Ultrathin SiO2 Films Grown by Low-Temperature Atmospheric Pressure Atomic Layer Deposition. *Appl. Surf. Sci.* **2020**, *530*, No. 147244.
(10) Liu, Y.; Ge, C.; Min, R.; et al. Effects of coating parameters on the morphology of SiO2-coated TiO2 and the pigmentary properties. *Appl. Surf. Sci.* **2008**, *254*, 2809−2819.
(11) Zhang, Y.; Yin, H.; Wang, A.; et al. Evolution of zirconia coating layer on rutile TiO2 surface and the pigmentary property. *J. Phys. Chem. Solids* **2010**, *71*, 1458−1466.
(12) Gao, H.; Qiao, B.; Wang, T. J.; et al. Effects of porous films on the light reflectivity of pigmentary titanium dioxide particles. *Appl. Surf. Sci.* **2016**, *387*, 581−587.
(13) Liang, Y.; Yu, K.; Xie, J.; Wang, T.; Zheng, Q. High hiding power and weather durability of film-coated titanium dioxide particles with a yolk-shell structure. *Colloids Surf., A* **2017**, *520*, 736−742.
(14) Wu, C.-Y.; Tu, K.; Deng, J.; et al. Markedly Enhanced Surface Hydroxyl Groups of TiO_2 Nanoparticles with Superior Water-Dispersibility for Photocatalysis. *Materials* **2017**, *10*, 566.
(15) Zhao, J.; Jie, Z.; Milanova, M.; Warmoeskerken, M. Surface modification of TiO_2 nanoparticles with silane coupling agents. *Colloids Surf., A* **2012**, *413*, 273−279.
(16) Wang, C.; Mao, H.; Wang, C.; Fu, S. Dispersibility and Hydrophobicity Analysis of Titanium Dioxide Nanoparticles Grafted with Silane Coupling Agent. *Ind. Eng. Chem. Res.* **2011**, *50*, 11930−11934.
(17) Ukaji, E.; Furusawa, T.; Sato, M.; Suzuki, N. The effect of surface modification with silane coupling agent on suppressing the photo-catalytic activity of fine TiO_2 particles as inorganic UV filter. *Appl. Surf. Sci.* **2007**, *254*, 563−569.
(18) Singh, J.; Gusain, A.; Saxena, V.; et al. XPS, UV−Vis, FTIR, and EXAFS Studies to Investigate the Binding Mechanism of N719 Dye onto Oxalic Acid Treated TiO_2 and Its Implication on Photovoltaic Properties. *J. Phys. Chem. C* **2013**, *117*, 21096−21104.
(19) Lowenstern, J. B.; Pitcher, B. W. Analysis of H_2O in silicate glass using attenuated total reflectance (ATR) micro-FTIR spectroscopy. *Am. Mineral.* **2013**, *98*, 1660−1668.
(20) Liu, F.; Zhi, L.; Gu, Y.; et al. Synthesis and characterization of a conducting polyaniline/TiO2−SiO2 composites. *J. Appl. Polym. Sci.* **2013**, *130*, 2288−2295.
(21) Song, X.; Gao, L. Synthesis, characterization, and optical properties of well-defined N-doped, hollow silica/titania hybrid microspheres. *Langmuir* **2007**, *23*, 11850−11856.
(22) Chen, Y.; Liu, K. Fabrication of Ce/N co-doped TiO2/diatomite granule catalyst and its improved visible-light-driven photoactivity. *J. Hazard. Mater.* **2017**, *324*, 139−150.
(23) Pinho, L.; Mosquera, M. J. Photocatalytic activity of TiO_2-SiO_2 nanocomposites applied to buildings: Influence of particle size and loading. *Appl. Catal., B* **2013**, *134*−*135*, 205−221.
(24) Kim, H. J.; Kang, I. G.; Kim, D. H.; Choi, B. H. Dispersion characteristics of TiO_2 particles coated with the SiO_2 nano-film by atomic layer deposition. *J. Nanosci. Nanotechnol.* **2011**, *11*, 10344−10348.
(25) Zhai, L.; Yan, W.; Feng, P.; et al. Synthesis of TiO_2−SiO_2/waterborne polyurethane hybrid with amino-siloxane terminated via a sol−gel process. *Mater. Lett.* **2012**, *89*, 81−85.
(26) Wang, L.; Hu, C. Y.; Yan, K. L. A one-step inkjet printing technology with reactive dye ink and cationic compound ink for cotton fabrics. *Carbohydr. Polym.* **2018**, *197*, 490−496.
(27) Han, Z.; Li, P.; Deng, Y.; Li, H. Reversible and color-variable afterglow luminescence of carbon dots triggered by water for multilevel encryption and decryption. *Chem. Eng. J.* **2021**, *415*, No. 128999.
(28) Zhao, H.; Hou, L.; Lu, Y. Electromagnetic shielding effectiveness and serviceability of the multilayer structured cuprammonium fabric/polypyrrole/copper (CF/PPy/Cu) composite. *Chem. Eng. J.* **2016**, *297*, 170−179.